

11313

MINISTERE DE LA POLITIQUE ET DE LA PROGRAMMATION SCIENTIFIQUE

CENTRE INTERUNIVERSITAIRE D'EXCELLENCE EN OCEANOGRAPHIE

(Actions Concertées)

THREE-DIMENSIONAL MODEL OF TIDES AND STORM SURGES

IN A SHALLOW WELL-MIXED CONTINENTAL SEA

by

Jacques C.J. NIHOUL

University of Liège, Belgium

Rapport ACN 1

## 1. Introduction

Although depth-integrated two-dimensional models of marine circulation are now very well established, very little has been done so far in the development of three-dimensional models. This is due, in particular, to the difficulty of solving three-dimensional time dependent equations and providing appropriate boundary conditions for them.

Integration over depth introduces, in the hydrodynamic equations, the surface stress and the bottom stress and, while the former can be evaluated from atmospheric data, the latter must be parameterized in terms of the mean or depth-integrated horizontal velocity introducing an empirical drag coefficient. In general, one sets (e.g. Groen and Groves 1966, Heaps 1967, Rind 1976)

$$(1) \quad \tau_b = -m \tau_s + D \bar{u} \|\bar{u}\|$$

where  $\tau_b$  and  $\tau_s$  are respectively the specific bottom and surface stresses (stresses divided by the specific mass of sea water) and where  $m$  and  $D$  are two empirical coefficients ( $D$  is the drag coefficient).

The parameters  $m$  and  $D$  must be adjusted not only to have the right magnitude of  $\tau_b$  but also the right direction. One notes that eq. (1), if used with constant  $m$  and  $D$ , introduces a rather severe assumption on the relationship between the direction of the bottom stress and that of the mean flow velocity  $\bar{u}$ . An error at this stage might seriously affect the final prediction of the model and several authors have stressed the need of three-dimensional modelling if only to assess the limits of validity of eq.(1).

In addition, the determination of the vertical profile of the horizontal velocity has, beside its obvious fundamental interest, a great importance in such applications as sediments transport, surface drift of pollutants... and it would help considerably in the interpretation of moored currentmeters data.

In this paper, a three-dimensional "long waves" model is discussed for the study of tides and storm surges in a shallow well-mixed continental sea. Emphasis is placed on the North Sea where tidal and storm currents constitute the essential part of the circulation and estimates from observation in the North Sea and, more especially, the Southern Bight are used to assess the relative importance of different effects and derive a simple set of equations by which vertical profiles of tidal and storm currents can be predicted, at each point, as functions of time.

## 2. Three-dimensional equations for tides and storm surges in a well-mixed shallow sea.

The three-dimensional equations describing tidal and storm currents in a well-mixed (constant density) shallow sea are fairly classical. If  $\underline{u} = (u_1, u_2, u_3)$  is the velocity vector,  $u_3$  denoting the vertical component and the vertical axis pointing upwards, they can be written (e.g. Nihoul 1975) :

$$(2) \quad \nabla \cdot \underline{u} = 0$$

$$(3) \quad \frac{\partial u_1}{\partial t} + \underline{u} \cdot \nabla u_1 - f u_2 = - \frac{\partial}{\partial x_1} \left( \frac{p_a}{\rho} + g \zeta \right) + \frac{\partial}{\partial x_3} \left( \tilde{v} \frac{\partial u_1}{\partial x_3} \right)$$

$$(4) \quad \frac{\partial u_2}{\partial t} + \underline{u} \cdot \nabla u_2 + f u_1 = - \frac{\partial}{\partial x_2} \left( \frac{p_a}{\rho} + g \zeta \right) + \frac{\partial}{\partial x_3} \left( \tilde{v} \frac{\partial u_2}{\partial x_3} \right)$$

where  $f$  is twice the vertical component of the earth's rotation vector,  $p_a$  is the atmospheric pressure,  $\rho$  the specific mass of sea water,  $\zeta$  the surface elevation and  $\tilde{v}$  the vertical eddy viscosity.

In these equations, the quasi-static approximation has been used to eliminate the pressure, the effect of the horizontal component of the earth's rotation vector (multiplied by  $u_3 \ll u_1$  or  $u_2$ ) has been ignored and the horizontal turbulent diffusion of momentum has been neglected as compared with the vertical diffusion; taking into account that horizontal length scales are much larger than the depth.

If

$$(5)(6) \quad x_3 = \zeta \quad \text{and} \quad x_3 = -h$$

are the equations of the free surface and the bottom, respectively, it is convenient to change variables to

$$(7) \quad \xi = \frac{x_3 + h}{H}$$

where

$$(8) \quad H = h + \zeta$$

is the total depth.

The new variable  $\xi$  varies from some very small value  $\xi_0 = \frac{z_0}{H}$  ( $z_0$  being the rugosity length) to 1 and the lower limit will be taken as zero as long as it does not create a singularity.

With this change of variable, the first two terms of the left-hand sides of (3) and (4) become

$$\frac{\partial u_i}{\partial t} + A_i + B_i + S_i \quad i = 1, 2$$

where

$$(9) \quad A_i = u_1 \frac{\partial u_i}{\partial x_1} + u_2 \frac{\partial u_i}{\partial x_2} \quad i = 1, 2$$

$$(10) \quad B_i = H^{-1} \frac{\partial u_i}{\partial \xi} (1 - \xi) (u_1 \frac{\partial h}{\partial x_1} + u_2 \frac{\partial h}{\partial x_2} + u_3) \quad i = 1, 2$$

$$(11) \quad S_i = H^{-1} \frac{\partial u_i}{\partial \xi} \xi \left( (u_{1s} - u_1) \frac{\partial \zeta}{\partial x_1} + (u_{2s} - u_2) \frac{\partial \zeta}{\partial x_2} - (u_{3s} - u_3) \right) \quad i = 1, 2$$

and where the relation

$$(12) \quad \frac{\partial \zeta}{\partial t} + u_{1s} \frac{\partial \zeta}{\partial x_1} + u_{2s} \frac{\partial \zeta}{\partial x_2} = u_{3s} \quad \text{at} \quad x_3 = \zeta$$

has been used, the subscripts denoting surface values.

To estimate the orders of magnitude of the non-linear terms A, B and S, one must have some, even rough, idea of the vertical profile of the velocity and, for that purpose, one can presumably take Van Veen's profile ( $u = u_s \xi^{0.2}$ ) which is probably not too good in the immediate vicinity of the bottom but appears to reproduce satisfactorily the observations in many cases (e.g. Bowden 1965, Nihoul 1975).

Now, the function  $(1 - \xi)\xi^{0.2}$  appearing in B is zero at the surface and at the bottom. Its larger values occur near the bottom (it has a maximum  $\sim 0.6$  for  $\xi \sim 0.17$ ). The function  $\xi(1 - \xi^{0.2})$  appearing in S is more evenly distributed over the water column but it remains small everywhere (it has a maximum  $\sim 0.06$  for  $\xi \sim 0.4$ ).

Comparing A and S (noting that  $u$  and  $\zeta$  have the same characteristic length of horizontal variations) one finds

$$\frac{S}{A} \sim \xi(1 - \xi^{0.2}) \frac{\zeta}{H}$$

Even in very shallow coastal zones, this can only be a few percents and one may reasonably neglect S as compared to A.

Dealing with long waves, one may associate to the time variations and the horizontal space variations of the velocity field a typical frequency  $\omega$  ( $\omega \sim 10^{-4} \sim f$ ) and a typical wave-length  $c/\omega$  where  $c$  is the phase velocity.

Observed values of the phase velocity exceed 10m/sec even in shallow coastal areas (note that  $\sqrt{gH}$  gives 10m/sec for  $H$  only 10 meters). Maximum values of the flow velocity  $u$  are of the order of 1m/sec. The non-linear advection term A (and a fortiori S) is thus generally negligible as compared to the time derivative; the two terms being in the ratio  $u/c$ .

This might not be true in some places, near amphidromic points, for instance where the characteristic length of horizontal variations of the velocity field could be smaller than the wave length. Its smaller value however is the grid size, because one cannot introduce in the model variations at scales which are meant to be smoothed out.

Still with a grid size of, say, 10 km, A could be one order of magnitude larger. A depth-integrated model should thus keep the non-linear advection term\*. Here, one is essentially interested in the vertical profile of the velocity and it seems reasonable to neglect A with the proviso that the model may not be valid in a few localized places.

The characteristic length of variations of the bottom topography  $h(x_1, x_2)$  is not related to the wave-length  $c/\omega$ . It cannot however be smaller than the grid size for the same obvious reason as before. For a 10 km grid size, each term composing B can be comparable to the time derivative. However, as shown previously, B is essentially important near the bottom where one may expect the streamlines to follow the bottom topography fairly closely. In that case, the three terms may be expected to nearly cancel each other, i.e.

$$(13) \quad u_1 \frac{\partial h}{\partial x_1} + u_2 \frac{\partial h}{\partial x_2} + u_3 \sim 0 \quad \text{near the bottom}$$

In the following, counting on a grid size of some 10 km and assuming that the departure of the left-hand side of (13) does not exceed 10 % of the value of the individual terms, one shall neglect B as compared to  $\frac{\partial u}{\partial t}$ . One should be aware, however, that, in finer grid models, for coastal studies for instance, B might be more important and, indeed, turn out to be the essential contribution of the non-linear terms to include by priority in the models.

Changing variables from  $x_3$  to  $\xi$ , the last terms in the right-hand sides of eq. (3) and (4) become

$$H^{-2} \frac{\partial}{\partial \xi} \left( \tilde{\nu} \frac{\partial u_i}{\partial \xi} \right) \quad i = 1, 2$$

Observations indicate that the eddy viscosity  $\tilde{\nu}$  can be expressed as the product of a function of  $t, x_1$  and  $x_2$  and a function of  $\xi$  (Bowden 1965). If one sets

$$(14) \quad \tilde{\nu} H^{-2} = \sigma(t, x_1, x_2) \lambda(\xi)$$

and neglects the non-linear terms according to the discussion above, one can write eq.(3) and (4) in the simple form :

\*-

It can be shown that they are also necessary if one wants to model correctly the residual circulation (Nihoul 1975).

$$(15) \quad \frac{\partial u_1}{\partial t} - f u_2 = - \frac{\partial}{\partial x_1} \left( \frac{p_a}{\rho} + g\zeta \right) + \sigma \frac{\partial}{\partial \xi} \left( \lambda \frac{\partial u_1}{\partial \xi} \right)$$

$$(16) \quad \frac{\partial u_2}{\partial t} + f u_1 = - \frac{\partial}{\partial x_2} \left( \frac{p_a}{\rho} + g\zeta \right) + \sigma \frac{\partial}{\partial \xi} \left( \lambda \frac{\partial u_2}{\partial \xi} \right)$$

### 3. Locally one-dimensional model of the vertical variations of the horizontal current

Let

$$(17) \quad u = u_1 + i u_2$$

$$(18) \quad \tau = \tilde{v} \frac{\partial u}{\partial x_3} = \sigma H \lambda \frac{\partial u}{\partial \xi}$$

$$(19) \quad \phi = - \frac{\partial}{\partial x_1} \left( \frac{p_a}{\rho} + g\zeta \right) - i \frac{\partial}{\partial x_2} \left( \frac{p_a}{\rho} + g\zeta \right)$$

eq (15) and (16) can be combined into the single equation

$$(20) \quad \frac{\partial u}{\partial t} + i f u = \phi + \sigma \frac{\partial}{\partial \xi} \left( \lambda \frac{\partial u}{\partial \xi} \right)$$

The forcing term  $\phi$  is a function of  $t$ ,  $x_1$  and  $x_2$ . Hence, although the dependence does not appear explicitly in eq. (20),  $u$  must be regarded as a function of  $\xi$ ,  $t$ ,  $x_1$  and  $x_2$ . At any given point  $x_1$ ,  $x_2$ , eq. (20) provides a locally one-dimensional model of the vertical distribution of  $u$  as a function of time.

If  $\tau_s$  and  $\tau_b$  denote the values of  $\tau$  at the surface and at the bottom respectively, the depth-averaged velocity  $\bar{u}$  is given by the equation

$$(21) \quad \frac{\partial \bar{u}}{\partial t} + i f \bar{u} = \phi + (\tau_s - \tau_b) H^{-1}$$

and the deviation  $\hat{u} = u - \bar{u}$  is given by

$$(22) \quad \frac{\partial \hat{u}}{\partial t} + i f \hat{u} = \sigma \left\{ \frac{\partial}{\partial \xi} \left( \lambda \frac{\partial \hat{u}}{\partial \xi} \right) - \frac{\tau_s - \tau_b}{\sigma H} \right\}$$

The vertical profile of the eddy viscosity  $\tilde{v}$  may be different in different circumstances but it is generally admitted that, in any case, its asymptotic behaviour for small  $\xi$  is given by

$$(23) \quad \tilde{v} = \kappa |\tau_b|^{1/2} (x_3 + h)$$

where  $\kappa$  is the Von Karman constant.

Combining (23) and (14), one finds

$$(24) \quad \sigma H = \kappa |\tau_b|^{1/2}$$

and

$$(25) \quad \lambda(\xi) \sim \xi \quad \text{for small } \xi$$

Changing variables to  $w$  and  $y$  defined by

$$(26) \quad \hat{u} = w e^{-i f t} + \frac{\tau_s}{\sigma H} s(\xi) + \frac{\tau_b}{\sigma H} b(\xi)$$

$$(27) \quad y = \int_0^t \sigma(v) dv$$

where

$$(28) \quad s(\xi) = \int_{\xi_0}^{\xi} \frac{\eta}{\lambda(\eta)} d\eta$$

$$(29) \quad b(\xi) = \int_{\xi_0}^{\xi} \frac{1 - \eta}{\lambda(\eta)} d\eta$$

eq. (22) can be written

$$(30) \quad \frac{\partial w}{\partial y} + \theta_s s(\xi) + \theta_b b(\xi) = \frac{\partial}{\partial \xi} \left( \lambda \frac{\partial w}{\partial \xi} \right)$$

where

$$(31) \quad \theta_\alpha = \frac{e^{i f t}}{\sigma} \left( \frac{\partial}{\partial t} + i f \right) \left( \frac{\tau_\alpha}{\sigma H} \right) = \frac{\partial}{\partial y} \left( e^{i f t} \frac{\tau_\alpha}{\sigma H} \right) \quad \alpha = s, b$$

with the boundary conditions

$$(32) \quad \lambda \frac{\partial w}{\partial \xi} = 0 \quad \text{at} \quad \xi = 0 \quad \text{and} \quad \xi = 1$$

If the vertical profile of the eddy viscosity is known  $s$  and  $b$  are known functions of  $\xi$ . One shall proceed considering  $\sigma$ ,  $H$ ,  $\theta_s$  and  $\theta_b$ , - at any given point  $x_1$ ,  $x_2$  -, as known functions of  $y$  hence of  $y$ . One can imagine for instance that a preliminary depth-integrated model has been solved for the marine region of interest; determining  $\sigma$ ,  $H$ ,  $\tau_s$  and  $\tau_b$  everywhere. Such a model would



of course rely on appropriate parameterization of  $\tau_b$  in terms of  $\bar{u}$  and the functions  $\sigma$ ,  $H$  ... given by this model should really be regarded as the starting point of an iteration process by which the results of the depth-dependent equations are used to improve the formulation of the depth-integrated model providing better estimates of  $\sigma$ ,  $H$ ,  $\tau_s$  and  $\tau_b$  etc...

#### 4. Vertical profile of the horizontal current

Introducing the Laplace transforms

$$(33) \quad W(a, \xi) = \int_0^{\infty} e^{-ay} w(y, \xi) dy$$

$$\Theta_{\alpha}(a) = \int_0^{\infty} e^{-ay} \Theta_{\alpha}(y) dy \quad \alpha = s, b$$

eq. (31) can be transformed into

$$(34) \quad aW + \Theta_s s(\xi) + \Theta_b b(\xi) - w_0(\xi) = \frac{d}{d\xi} \left( \lambda \frac{dW}{d\xi} \right)$$

with the boundary conditions

$$(35) \quad \lambda \frac{dW}{d\xi} = 0 \quad \text{at } \xi = 0 \quad \text{and } \xi = 1$$

Let now a series of functions  $f_n(\xi)$  ( $n = 0, 1, \dots$ ) such that

$$(36) \quad \frac{d}{d\xi} \left( \lambda \frac{df_n}{d\xi} \right) = -\alpha_n f_n \quad n = 0, 1, 2, \dots$$

$$(37) \quad \lambda \frac{df_n}{d\xi} = 0 \quad \text{at } \xi = 0 \quad \text{and } \xi = 1$$

The  $\alpha_n$ 's being appropriate eigenvalues with  $\alpha_0 = 0$ .

It is readily seen that these functions are orthogonal on  $(0, 1)$ . They can be further normalized by imposing

$$(38) \quad \int_0^1 f_n^2 d\xi = 1$$

It is tempting to seek a solution of (34) in the form of a series expansion in  $f_n(\xi)$ . This is somewhat similar to the method used by Heaps (1972) in an earlier very attractive endeavour of three-dimensional modelling, although the setting here is not quite the same and the eigenfunctions are different.

Let thus

$$(39) \quad W = \sum_{n=0}^{\infty} c_n f_n(\xi)$$

$$(40) \quad w_o = \sum_{n=0}^{\infty} \omega_n f_n(\xi)$$

$$(41) \quad s = \sum_{n=0}^{\infty} s_n f_n(\xi)$$

$$(42) \quad b = \sum_{n=0}^{\infty} b_n f_n(\xi)$$

The coefficients  $\omega_n$ ,  $s_n$ ,  $b_n$  are known if  $\lambda(\xi)$  and thus  $s(\xi)$  and  $b(\xi)$  are known. The coefficients  $c_n$  are determined by (34). One finds

$$(43) \quad c_n = \frac{\omega_n - s_n \Theta_s - b_n \Theta_b}{a + \alpha_n}$$

Hence

$$(44) \quad w = \mathcal{L}^{-1} W = \sum_{n=0}^{\infty} \left\{ \omega_n e^{-\alpha_n y} - s_n R_n^s - b_n R_n^b \right\} f_n(\xi)$$

where

$$(45) \quad R_n^\alpha = \int_0^y \Theta_\alpha(y') e^{-\alpha_n(y-y')} dy' \quad \alpha = s, b$$

From (36) and (37), it is readily seen that

$$(46) \quad \int_0^1 f_n(\xi) d\xi = 0 \quad n > 0$$

and that  $f_0$  is a constant so that the first terms in the series expansions (39) (40) (41) and (42) represent the depth-mean values of the corresponding functions.

Combining (26), (31) and (44), one then obtains

$$(47) \quad \hat{u} = \frac{\tau_s}{\sigma_H} (s(\xi) - \bar{s}) + \frac{\tau_b}{\sigma_H} (b(\xi) - \bar{b}) \\ + \sum_{n=1}^{\infty} \left\{ \omega_n e^{-\alpha_n y} - s_n R_n^s - b_n R_n^b \right\} f_n(\xi)$$

By successive integrations by parts, one can write, using (31)

$$\begin{aligned}
 (48) \quad R_n^\alpha &= \sum_{p=0}^{\infty} \left( \frac{d^p \theta_\alpha}{dy^p} \frac{e^{\alpha_n y}}{\alpha_n^{p+1}} \right)_0 e^{-\alpha_n y} & \alpha &= s, p \\
 & & n &= 1, 2, \dots \\
 &= \sum_{q=1}^{\infty} \left\{ \alpha_n^{-q} \frac{d^q}{dy^q} \left( \frac{e^{ift \tau_\alpha}}{\sigma H} \right) - \alpha_n^{-1} e^{-\alpha_n y} \left( \frac{d^q}{dy^q} \left( \frac{e^{ift \tau_\alpha}}{\sigma H} \right) \right)_0 \right\}
 \end{aligned}$$

Values of  $\sigma$  in the North Sea may vary from  $10^{-4} \text{ sec}^{-1}$ , in cases of small currents almost reduced to residual at turning tides and weak winds, to  $10^{-2} \text{ sec}^{-1}$  in cases of large tidal currents and strong winds. The time variations of the stress and velocity fields may be characterized by a typical "frequency"  $\omega \sim 10^{-4} \text{ sec}^{-1} \sim f$ .

Thus

$$\frac{d}{dy} = \frac{1}{\sigma} \frac{d}{dt} \sim \frac{\omega}{\sigma} \lesssim 1$$

Successive differentiations with respect to  $y$  should thus, if anything, reduce the order of magnitude. The eigenvalues  $\alpha_n$  being increasing functions of  $n$ , the factors  $\alpha_n^{-q}$  in (48) will rapidly become negligibly small as  $n$  and  $q$  increase and one foresees that in (47) and (48), only a few terms of the sums will have to be retained.

With the observed values of  $\sigma$ , the variable  $y$  reaches values of order 10 in less than a tidal period. One can see then that the influence of the initial conditions rapidly vanishes; the factor  $e^{-\alpha_n y}$  (in 47 and 48) becoming exceedingly small.

Thus, after a short time, the essential contribution to the velocity deviation will be

$$\begin{aligned}
 (49) \quad \hat{u} &= \frac{\tau_s}{\sigma H} (s(\xi) - \bar{s}) + \frac{\tau_b}{\sigma H} (b(\xi) - \bar{b}) \\
 &- \sigma^{-1} \frac{\partial}{\partial t} \left\{ \frac{e^{ift}}{\sigma H} \left( \frac{s_1 \tau_s + b_1 \tau_b}{\alpha_1} \right) \right\} f_1(\xi)
 \end{aligned}$$

One can see that Ekman veering affects only the third term (and the other smaller terms of the sum) and is most effective when  $\sigma$  is the smallest (low current velocities, weak winds) as one would normally expect.

It is illuminating at this stage to consider a single example.

The observations indicate that the eddy viscosity increases first linearly with height over the bottom, and then flattens out in the upper layers following some form of parabolic curve (e.g. Bowden 1965).

It thus appears that  $\lambda$  could be reasonably well represented by a law of the form

$$(50) \quad \lambda = \xi \left(1 - \frac{1}{2} \xi\right)$$

behaving as  $\xi$  for small values of  $\xi$  and increasing to a maximum value at  $\xi = 1$ .

The corresponding eigenfunctions and eigenvalues are found to be

$$(51) \quad f_n = (4n + 1)^{1/2} P_{2n}(\xi - 1)$$

$$(52) \quad \alpha_n = n(2n + 1)$$

where  $P_{2n}$  denotes the Legendre polynomials of even order.

Eq. (49) becomes

$$(53) \quad \begin{aligned} \hat{u} = & \frac{\tau_s}{\sigma H} (4 \ln 2 - 2 - 2 \ln (2 - \xi)) \\ & + \frac{\tau_b}{\sigma H} (2 - 2 \ln 2 + \ln (2 - \xi) + \ln \xi) \\ & + \sigma^{-1} \frac{\partial}{\partial t} \left( e^{ift} \frac{\tau_s + 2\tau_b}{\sigma H} \right) \left( \frac{5}{12} \xi^2 - \frac{5}{6} \xi + \frac{5}{18} \right) \end{aligned}$$

where it is understood that  $\xi$  runs from 0 to 1 everywhere except in  $\ln \xi$  where its lower limit must be specifically set at  $\xi_0$ .

At  $\xi = \xi_0 \sim 0$  one must have  $\hat{u} = -\bar{u}$ , i.e.

$$(54) \quad \begin{aligned} \bar{u} = & \frac{\tau_s}{\sigma H} (2 - 2 \ln 2) + \frac{\tau_b}{\sigma H} (-\ln \xi_0 + \ln 2 - 2) \\ & + \frac{5}{18} \sigma^{-1} \frac{\partial}{\partial t} \left( e^{ift} \frac{\tau_s + 2\tau_b}{\sigma H} \right) \end{aligned}$$

Hence

$$\begin{aligned}
 (55) \quad u = & \frac{\tau_s}{\sigma H} 2 \ln \frac{2}{2 - \xi} + \frac{\tau_b}{\sigma H} \left( \ln \xi / \xi_0 + \ln \frac{2 - \xi}{2} \right) \\
 & - \sigma^{-1} \frac{\partial}{\partial t} \left( e^{ift} \frac{\tau_s + 2 \tau_b}{\sigma H} \right) \frac{5}{12} \xi (2 - \xi)
 \end{aligned}$$

## 5. Parameterization of the bottom stress

Eq. (49) shows that the vertical profile of the velocity  $u$  is the result of three contributions which may be related to the wind stress, the bottom stress and the effect of the Coriolis force combined with the action of wind or bottom friction.

Using eq. (55) to estimate orders of magnitude, one finds (taking  $\ln \xi_0 = -10$  as a typical value) :

$$\begin{aligned}
 \frac{\frac{\tau_s}{\sigma H} 2 \ln \frac{2}{2 - \xi}}{\frac{\tau_b}{\sigma H} \left( \ln \xi / \xi_0 + \ln \frac{2 - \xi}{2} \right)} & \sim 0.1 \frac{\tau_s}{\tau_b} \\
 \frac{\sigma^{-1} \frac{\partial}{\partial t} \left( e^{ift} \frac{\tau_s}{\sigma H} \right) \frac{5}{12} \xi (2 - \xi)}{\frac{\tau_s}{\sigma H} 2 \ln \frac{2}{2 - \xi}} & \sim 0.3 \frac{\omega}{\sigma} \\
 \frac{\sigma^{-1} \frac{\partial}{\partial t} \left( e^{ift} \frac{\tau_b}{\sigma H} \right) \frac{5}{12} \xi (2 - \xi)}{\frac{\tau_b}{\sigma H} \left( \ln \xi / \xi_0 + \ln \frac{2 - \xi}{2} \right)} & \lesssim 0.1 \frac{\omega}{\sigma}
 \end{aligned}$$

where  $\omega$  is, as before, a typical frequency of time variations ( $\omega \sim 10^{-4} \text{ sec}^{-1} \sim f$ ).

- i) In the case of strong winds ( $> 10 \text{ m/sec}$ ) and strong currents ( $> 1 \text{ m/sec}$ ),  $\tau_s$  and  $\tau_b$  are comparable ( $\sim 10^{-3} \text{ m}^2/\text{sec}^{-2}$ ),  $\sigma$  can be one order of magnitude larger than  $\omega$ , the essential contribution is due to bottom friction, the direct effect of the wind stress does not exceed some 10 % of the former and there is no noticeable Ekman veering. This will be a fortiori true in the case of strong (tidal) currents and weak winds.

- ii) In the case of strong winds but relatively moderate currents related to residual and wind-induced circulations at slack tide, the effects of wind and bottom friction may become comparable. The Ekman veering will however remain rather limited as the ratio  $\omega/\sigma$  will presumably still be smaller than 1.
- iii) In the case of weak wind and small currents (almost reduced to residuals at slack tide), ( $\tau_s \sim \tau_b \sim 10^{-5}$ ) the essential contribution remains related to the bottom stress,  $\sigma$  may be comparable to  $\omega$  and both the wind stress and the Coriolis force can produce a 10 % deviation of the vertical profile of velocity.

Thus, in a shallow continental sea like the North Sea where tides are omnipresent and can reach velocities of the order of 1 m/sec or more, one expects that, during a substantial fraction of the tidal period, Coriolis effects may be neglected and eq. (54) can be written, in first approximation,

$$(56) \quad \bar{u} \sim \frac{\tau_s}{\sigma H} (2 - 2 \ln 2) + \frac{\tau_b}{\sigma H} (-\ln \xi_0 + \ln 2 - 2)$$

Moreover, the numerical coefficient of the first term being approximately 0.1 of the coefficient of the second term, eq. (24) may be written

$$(57) \quad (\sigma H)^2 = \kappa^2 |\tau_b| \sim \frac{\sigma H |\bar{u}| \kappa^2}{-\ln \xi_0 + \ln 2 - 2}$$

or

$$(58) \quad \sigma H \sim \frac{|\bar{u}| \kappa^2}{-\ln \xi_0 + \ln 2 - 2}$$

Combining with (56), one gets

$$(59) \quad \tau_b \sim -m \tau_s + D \bar{u} |\bar{u}|$$

or, equivalently

$$(59') \quad \tau_b \sim -m \tau_s + D \bar{u} \|\bar{u}\|$$

where

$$(60) \quad m = \frac{2 - 2 \ln 2}{-\ln \xi_0 + \ln 2 - 2} \sim 0.07$$

$$(61) \quad D = \frac{\kappa^2}{(-\ln \xi_0 + \ln 2 - 2)} \sim 2.11 \cdot 10^{-3} \quad \text{for } \ln \xi_0 \sim -10$$

Eq. (59) is identical with the empirical formula (1). Moreover the numerical values of the coefficients  $m$  and  $D$  predicted by the model appear in close agreement with the empirical coefficients used in success in practice ( $m \sim 0.1$ ,  $D \sim 2 \cdot 10^{-3}$ , Roday 1976).

The empirical bottom friction law (1) would thus seem to be valid except perhaps for a fraction of time of the tidal period.

Whether this is sufficient to affect significantly the predictions of a depth-integrated model and the determination of vertical profiles by the method developed in this paper and based on a preliminary calculation of  $\tau_b$ , remains to be verified. In any case, one can visualize an iteration process by which eq. (49) is used to recalculate the mean velocity field with a more appropriate  $\tau_b$  and the results used to derive improved vertical profiles, repeating the process until satisfactory convergence is obtained.

## 6. References

- Bowden K.F., (1965), Horizontal mixing in the sea due to a shearing current, J. Fluid Mech., 21, 83-95.
- Groen P. and Groves G.W. (1966), Surges, in The Sea, Vol. 1, edited by N. Hill, Interscience Publishers, Wiley N.Y. 611-646.
- Heaps N.S., (1967), Storm Surges, in Oceano. Mar. Biol. Ann. Rev. edited by H. Barnes, Allan and Unwin Publ. London 11-47.
- Heaps N.S., (1972), On the numerical solution of the three-dimensional hydrodynamical equations for tides and storm surges. Mém. Soc. Sc. Lg., 6, 143-180.
- Nihoul J.C.J., (1975), Modelling of Marine Systems, Elsevier Publ. Amsterdam.
- Roday F.C., (1976), Modèles hydrodynamiques. Rapport Final. Programme National Belge sur l'Environnement - Projet Mer Vol. 3.

## 7. Appendix

### Application of the three-dimensional model

Eqs (49) and (54) give the vertical profile of the horizontal velocity at any given point of the marine system knowing the results of the depth-integrated two-dimensional model and the form of the eddy viscosity .

With a good approximation, a parabolic profile can be fitted to represent  $\lambda$  and the vertical profile of the horizontal velocity is given by eq.(55). This approximation is valid everywhere in the North Sea except in some localized area where the vicinity of an amphidromic point, the proximity of the coast or the existence of a slight vertical or horizontal stratification may eventually invalidate the hypotheses made. In particular one should expect that in a fine grid coastal circulation model, the non-linear effects related to the variations of bottom topography, might be important and a specific non-linear three-dimensional coastal model is now being developed and prepared for a subsequent publication.

To illustrate the three-dimensional model, the vertical profile of the horizontal tide and storm surge velocity vector has been computed at the point 51°50'North 2°55'East under strong wind conditions where the two-dimensional depth-integrated model provided the following estimates

$$\|\bar{u}\|_{\sim} < 0.8 \text{ m sec}^{-1}$$

$$H \sim 45 \text{ m}$$

$$z_0 \sim 2.7 \cdot 10^{-3} \text{ m}$$

$$D \sim 2.2 \cdot 10^{-3}$$

$$\|\tau_s\| \sim 2.3 \cdot 10^{-4} \text{ m sec}^{-2}$$



Fig. 1 and Fig. 2 show the time evolution every hour over half a tidal period of the vertical profiles of the two horizontal components of the velocity vector.

Fig. 3 and Fig. 4 show the vertical profiles of  $u_1$  and  $u_2$  every 20' at tide reversal; illustrating the possibility of inverse flows in the upper and bottom layers during a short period of time.

Fig. 5 shows a comparison between the mean velocity computed by the three-dimensional model and the two-dimensional depth-integrated model respectively ; demonstrating the consistency of the two models and the quality of the three-dimensional modelling results.

dashed line : two dimensional model

full line : three dimensional model.

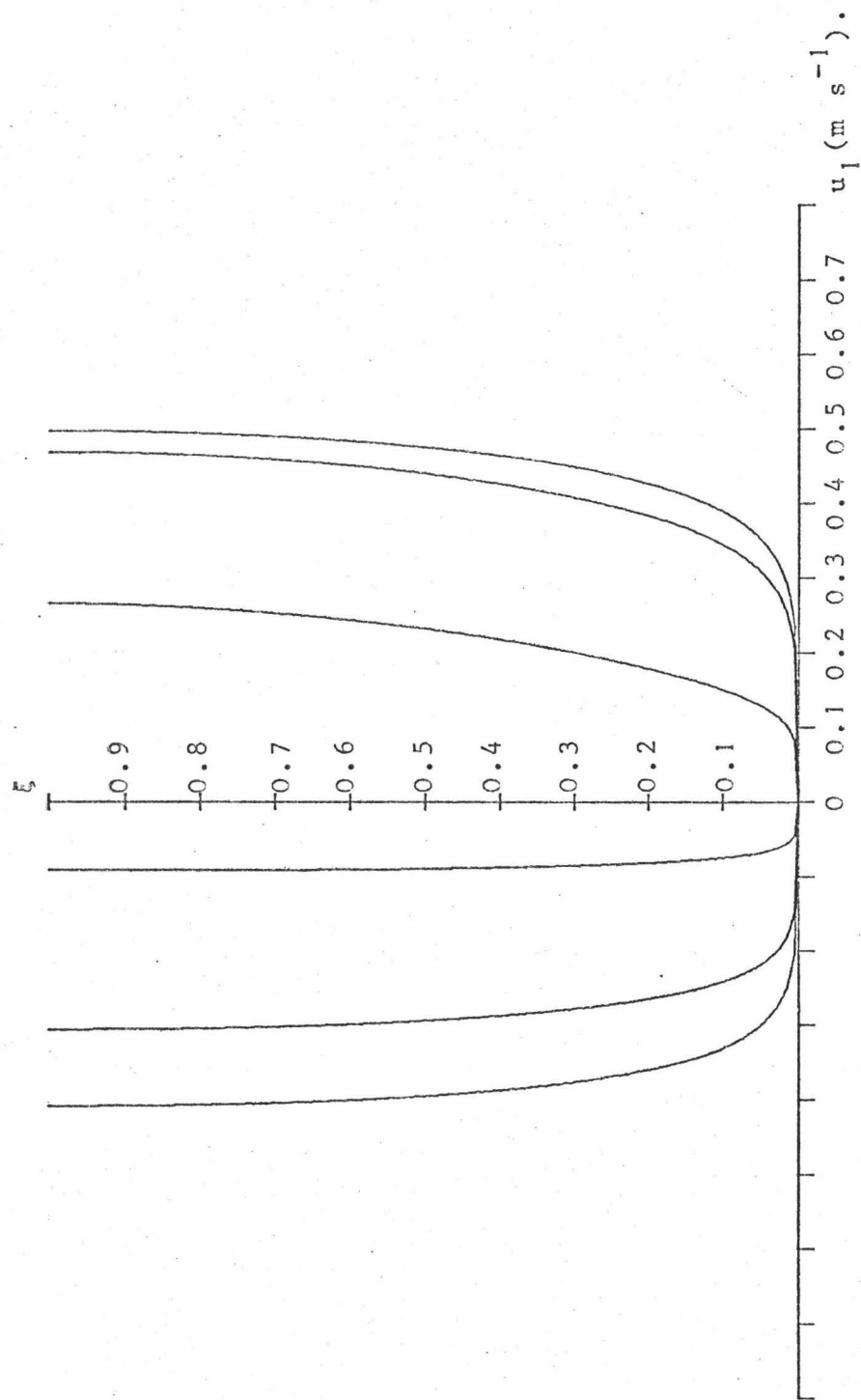


FIG. 1.

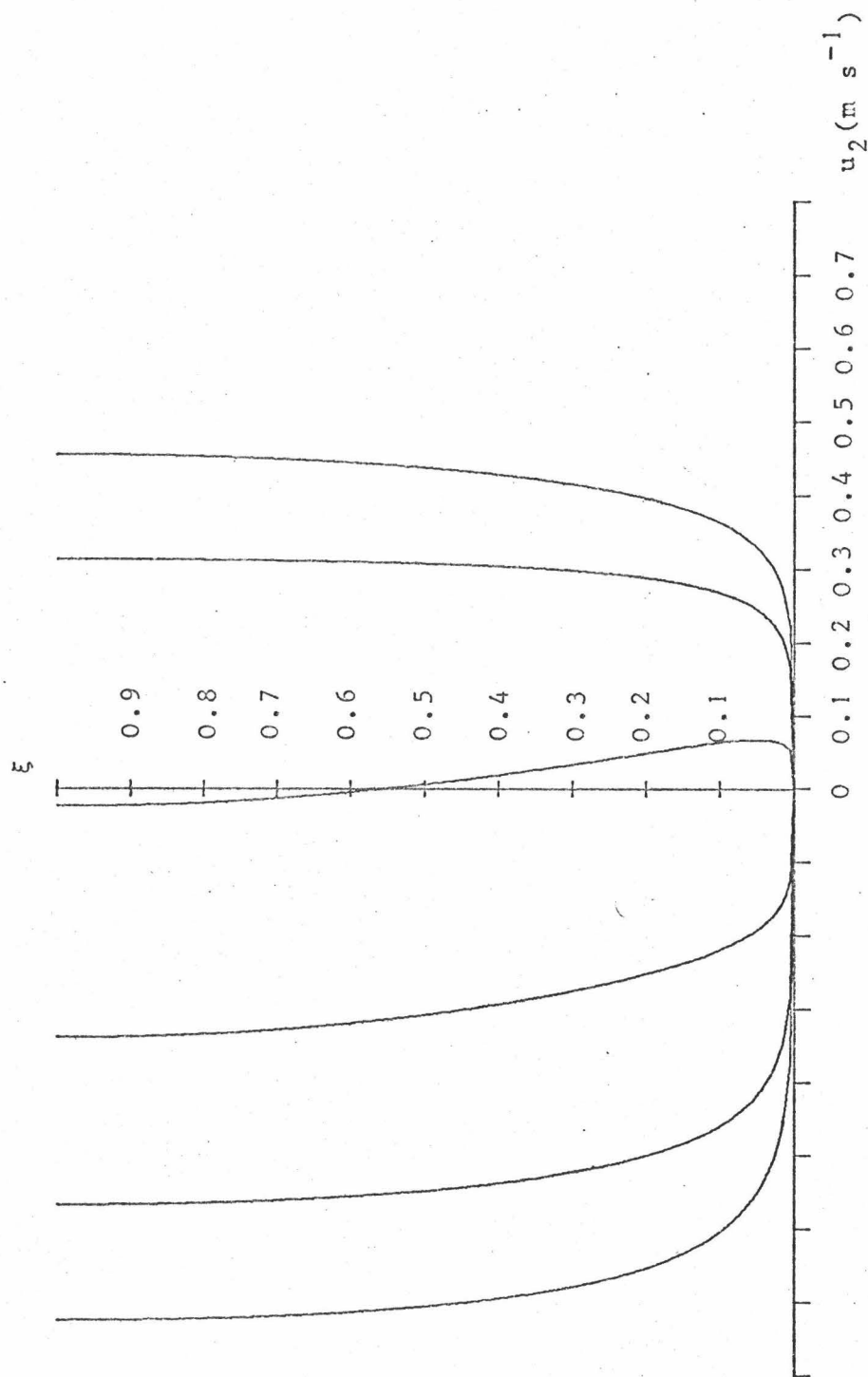


FIG. 2.

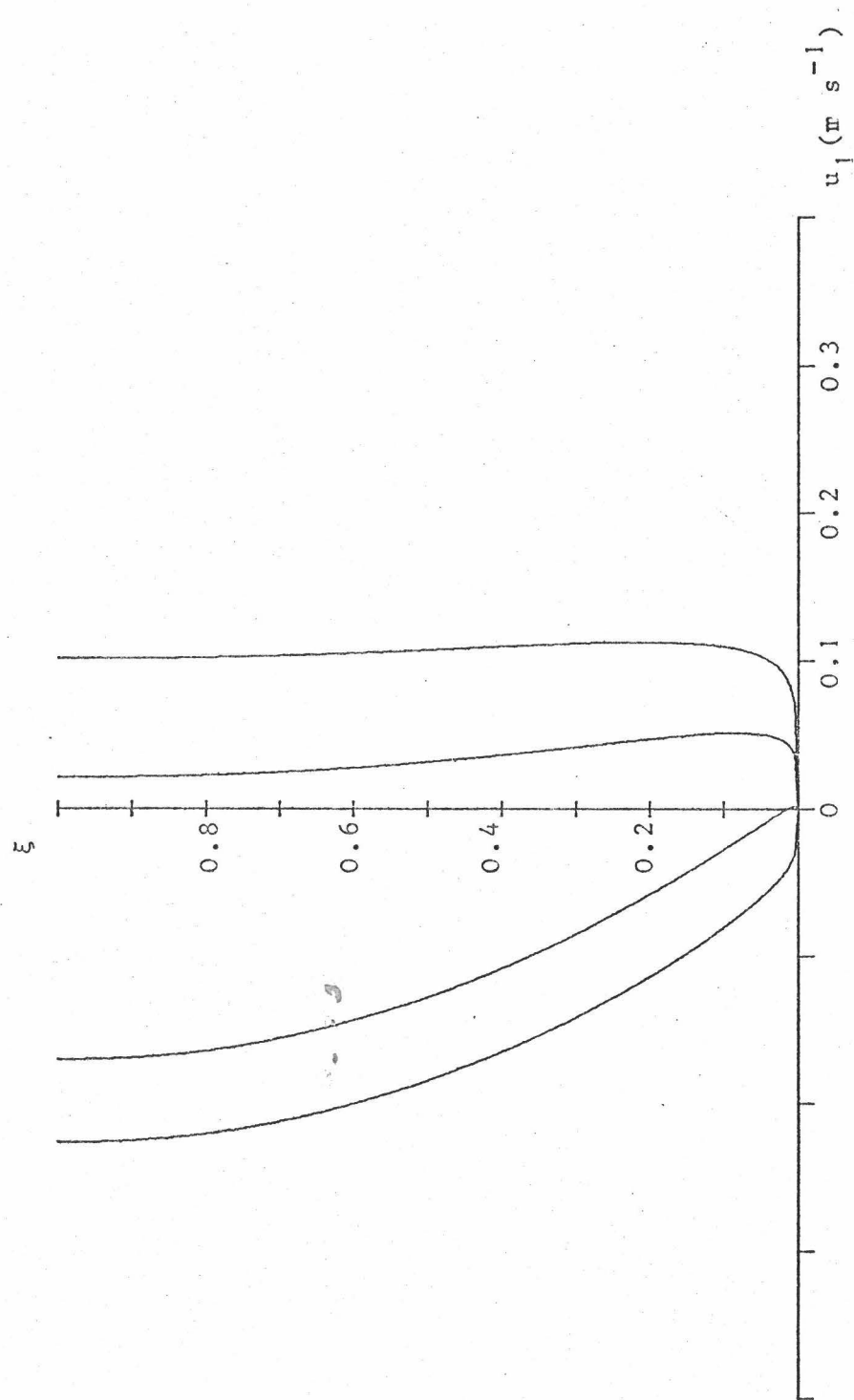


FIG. 3.

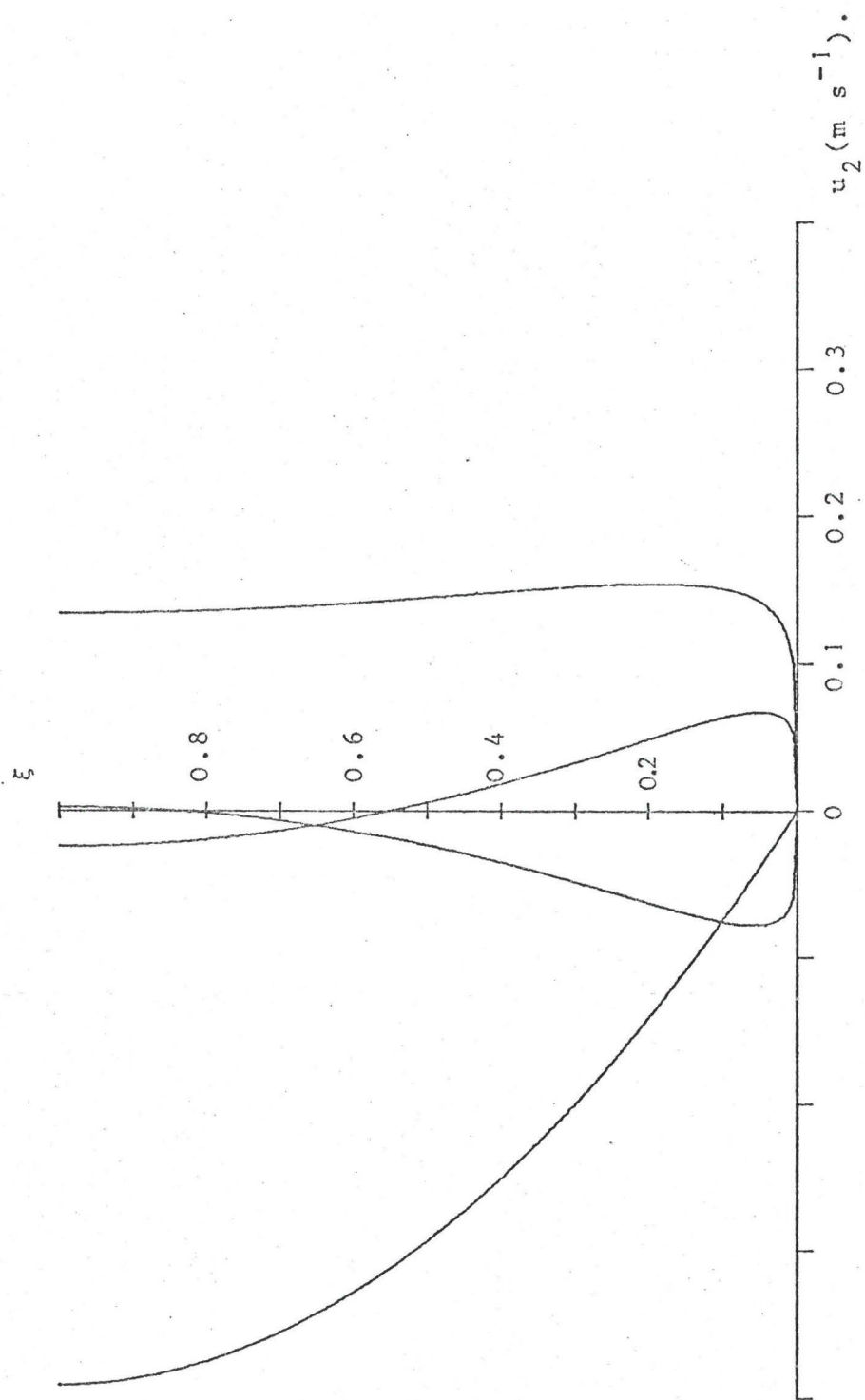


FIG. 4.

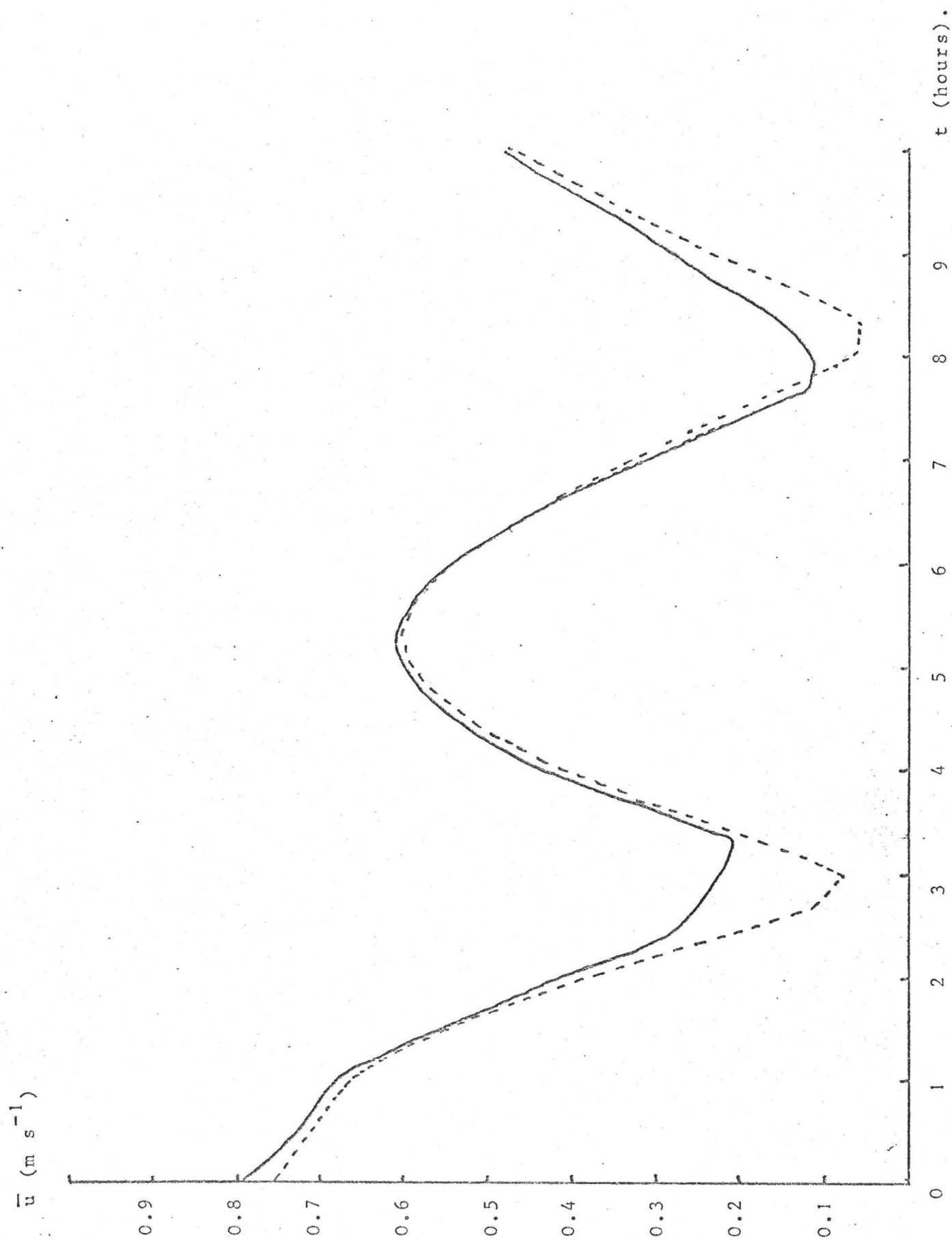


FIG. 5.